

# Porous ZnMnO<sub>3</sub> plates prepared from Zn/Mn–sucrose composite as high-performance lithium-ion battery anodes

Chenhao Zhao<sup>1,2</sup> ✉, Zhaoguo Teng<sup>1</sup>, Dan'ni Zhao<sup>1</sup>, Zhibiao Hu<sup>1,2</sup>, Kaiyu Liu<sup>1,2</sup>

<sup>1</sup>College of Chemistry and Materials Science, LongYan University, Fujian LongYan 364012, People's Republic of China

<sup>2</sup>Fujian Provincial Key Laboratory of Clean Energy Materials, LongYan University, Fujian LongYan, 364012, People's Republic of China

✉ E-mail: zhaochenhao123456@163.com

Published in Micro & Nano Letters; Received on 5th May 2016; Revised on 2nd June 2016; Accepted on 7th June 2016

Porous ZnMnO<sub>3</sub> plates have been prepared by an initial formation of Zn/Mn–sucrose composite and subsequent calcination route. The influences of calcination temperatures on the structures and electrochemical performances of target ZnMnO<sub>3</sub> are clearly studied. At an optimal calcination temperature of 500°C, the ZnMnO<sub>3</sub> composed of numerous nanoparticles possesses an obvious plate-like structure and porous property, and a Brunauer–Emmett–Teller specific surface area of ~25.50 m<sup>2</sup> g<sup>-1</sup> and average pore size of ~19.69 nm can be reached. As lithium-ion battery anode, the optimal ZnMnO<sub>3</sub> delivers a reversible (second) discharge capacity of 709.6 mAh g<sup>-1</sup> at 0.4 A g<sup>-1</sup>. After 100 cycles, a discharge capacity of 560.0 mAh g<sup>-1</sup> can be retained. Even at a high current density of 1.2 A g<sup>-1</sup>, the sample still shows a discharge capacity of 403.1 mAh g<sup>-1</sup>. The good electrochemical performance of as-prepared ZnMnO<sub>3</sub> may be attributed to its unique porous structure.

**1. Introduction:** Anode materials with high capacity, low voltage and cost have been regarded as one of the most important elements for high-performance lithium-ion battery [1, 2]. Transition metal oxides have been given much attention due to their high discharge capacity (500–1000 mAh g<sup>-1</sup>) compared with commercial graphite materials (372 mAh g<sup>-1</sup>) [3–5]. Among these conversion type metal oxides, the binary Mn-based oxide ZnMn<sub>2</sub>O<sub>4</sub> has a low voltage plateau and good cycling stability, which is favourable to give more energy at a whole cell. Furthermore, the environment benign and low costs of raw material suggest the Mn-based oxides have a potential application prospect [6–13]. As an analogy to ZnMn<sub>2</sub>O<sub>4</sub>, the ZnMnO<sub>3</sub> with cubic phase has same element composition with ZnMn<sub>2</sub>O<sub>4</sub>, and it also may possess good electrochemical performances [14–16]. In our previous study, the porous ZnMnO<sub>3</sub> microsphere has been prepared by decomposition of binary Zn–Mn carbonate. As lithium-ion battery anode, this porous microsphere delivers an initial discharge capacity of 1294 mAh g<sup>-1</sup> at 500 mA g<sup>-1</sup> and retains a reversible value of 879 mAh g<sup>-1</sup> even over 150 cycles [16].

However, the serious volume change and poor electrochemical conductivity of transition metal oxides, including ZnMnO<sub>3</sub> deeply affect their possible practical application [3–5]. In order to overcome these drawbacks, the construction of porous metal oxides has been regarded as one of most promising research directions [2–5]. Therein, the porous structure can buffer the volume change and provide short Li ion/electron diffusion pathways during cycling, and the excellent electrochemical performances can be expected. Taking similar ZnMn<sub>2</sub>O<sub>4</sub> as an example, the porous ZnMn<sub>2</sub>O<sub>4</sub> microspheres decomposed from corresponding Zn–Mn carbonate preserve a discharge capacity of 800 mAh g<sup>-1</sup> at a high current density of 500 mA g<sup>-1</sup> after 300 cycles [13].

It is still a challenge that how to prepare porous binary metal oxides due to their complex chemical compositions [17]. In previous study, the route with the initial formation of metal ion-organic molecule composite and subsequent decomposition has been widely used to prepare metal oxides, especially binary metal oxides [2, 12, 17–19]. Generally speaking, the metal ions can be uniformly dispersed with an organic molecule, and the decomposition of an organic molecule can induce the formation of porous structure. For example, Qiu *et al.* have prepared ZnCo<sub>2</sub>O<sub>4</sub> porous

nanoplate using Zn–Co ethylene glycol as precursor [19]. Porous ZnMn<sub>2</sub>O<sub>4</sub> nanocrystals were prepared using co-precipitation synthesised Zn–Mn citric complex as precursor [12]. Consideration of the fact that, the sucrose can form brown viscous solution, then fluffy bubble structure at a high temperature in the presence of nitrate (NO<sub>3</sub><sup>-</sup>) [20–22], the metal ion can be well dispersed in the sucrose-based matrix. In this Letter, the stoichiometries Zn(NO<sub>3</sub>)<sub>2</sub> and Mn(NO<sub>3</sub>)<sub>2</sub> are added into sucrose solution to induce the formation of Zn/Mn–sucrose composite at a high temperature, and the ZnMnO<sub>3</sub> can be prepared after subsequent high-temperature calcination. As lithium-ion battery anodes, the structures and electrochemical performances of different ZnMnO<sub>3</sub> are comparatively studied, and discussed clearly in this Letter.

**1.1. Synthesis of porous ZnMnO<sub>3</sub> plates:** The ZnMnO<sub>3</sub> was prepared by an initial formation of Zn/Mn–sucrose composite and subsequent decomposition, described as follows: 2.2311 g Zn(NO<sub>3</sub>)<sub>2</sub>·6H<sub>2</sub>O, 2.6843 g Mn(NO<sub>3</sub>)<sub>2</sub> (50 wt% in solution) and 1.198 g sucrose were dissolved into 5 ml distilled water in a 100 ml beaker. Then, the solution was kept at 140°C for 2–4 h until a fluffy bubble-like structure can be obtained. After grinding to powder, the prepared Zn/Mn–sucrose composite was annealed at 400, 500, 600 or 700°C to obtain porous ZnMnO<sub>3</sub> plate.

**1.2. Structural characterisation:** The crystal phases were measured on a powder X-ray diffractometer (DX-2700, Dandong) with Cu-Kα radiation (40 kV, 30 mA) and 0.03°/s in the 2θ range of 10° and 80°. The morphologies and sizes were observed using JEOL JSM-7600F Scanning Electron Microscope (SEM, 5 kV) and JEM-100CX11 Transmission Electron Microscope (TEM, 100 kV). Specific surface area and corresponding pore size of 500°C prepared ZnMnO<sub>3</sub> sample were measured using a Micromeritics ASAP 2020 sorptometer under N<sub>2</sub> atmospheres at 77 K.

**1.3. Electrochemical measurement:** CR 2016 coin cells were used for electrochemical experiments performed at room temperature. The electrode material, acetylene black and binder sodium alginate were mixed in an agate mortar at a weight ratio of 8:1:1. The resulting mixtures were transformed into a ceramic boat,

slurried with deionised water, pasted onto copper foils, and then dried at 80°C for 5–10 h. The dried electrode was cut into discs with a diameter of 14 mm. The cells were assembled in an argon-filled glove box using polymer (Celgard 2400) and commercial LBC 301 LiPF<sub>6</sub> solution (ShenZhen CAPCHEM) as separator and electrolyte, respectively. The galvanostatic cycling tests were conducted on a CT-3008 battery test system (ShenZhen Neware) at various current rates between 0.01 and 3.0 V.

**2. Results and discussion:** The ZnMnO<sub>3</sub> is prepared by an initial formation of Zn/Mn–sucrose composite and subsequent calcination route. At the beginning, the nitrate (NO<sub>3</sub><sup>-</sup>) can react with sucrose by redox reaction at a high temperature (i.e. 140°C), and a great amount of gases (NO<sub>x</sub> and CO<sub>x</sub>) can be produced [20–22]. Accompanying with the evaporation of H<sub>2</sub>O, the strong interaction (hydrogen bond) of sucrose molecule will result in the formation of brown viscous solution then fluffy bubble structure. Importantly, the metal ions Zn and Mn in the bubble-like composite can have uniformly dispersion, even at atomic level. Then, the obtained composite is ground into powder, and annealed at a certain temperature to obtain target ZnMnO<sub>3</sub>.

Fig. 1a reveals thermogravimetric analysis (TGA)–differential scanning calorimetry (DSC) curves of Zn/Mn–sucrose composite recorded from room temperature to 750°C at a heating rate of 10°C/min. The weight loss before 250°C may be attributed to the loss of moisture and adsorbed water. Subsequently, the huge weight loss of about 47.6% with an exothermic peak of 283.1°C is the combustion of residual sucrose and other organic (originated from sucrose). Interestingly, a minor weight loss occurs nearby 450°C may be the further phase transformation of metal oxides [23].

According to the TGA–DSC curves and previous reports [14–16], the calcination temperatures of Zn/Mn–sucrose are fixed as 400, 500, 600 or 700°C to obtain ZnMnO<sub>3</sub>, and corresponding XRD patterns are revealed in Fig. 1b. It can be seen that the sample obtained from low temperature (i.e. 400°C) has weak diffraction peaks, suggesting this sample has poor crystallinity. Worse still, partial diffraction peaks cannot be indexed to pure phase ZnMnO<sub>3</sub> (JCPDS Card No. 19–1461) [14–16]. With an increased temperature of 500°C, all of diffraction peaks of prepared sample can be indexed to standard ZnMnO<sub>3</sub>, and without any impurities can be detected. This transformation may be related to minor weight loss occurs nearby 450°C (Fig. 1a), suggesting the formation of ZnMnO<sub>3</sub> needs a temperature above 450°C. When the temperature further increases to 600 or higher 700°C, the sharper and narrower ZnMnO<sub>3</sub> diffraction peaks are found, indicating the samples have higher crystallinity and larger particle size [24].

The morphology of ZnMnO<sub>3</sub> obtained from 500°C is revealed in Fig. 2. In an overall view (Fig. 2a), some thick plate-like structure can be found, and these plates have a wide size distribution range from a few micrometres to tens of micrometres. In a magnification view, it can be seen the plate is very loose, and much macropore can be found on the surface. Consideration of loose precursor

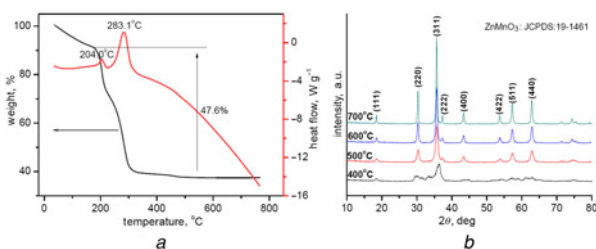


**Fig. 1** Zn/Mn–sucrose composite recorded from room temperature to 750°C at a heating rate of 10°C/min  
a TGA–DSC curves of Zn/Mn–sucrose composite recorded from room temperature to 750°C  
b XRD patterns of ZnMnO<sub>3</sub> obtained from different temperatures

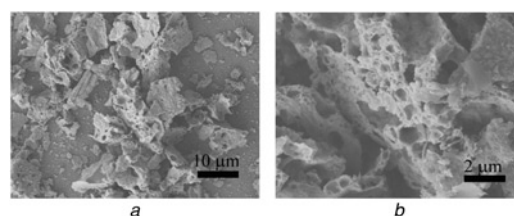


**Fig. 2** SEM images of 3D network porous ZnMnO<sub>3</sub> obtained from 500°C  
a Overall view  
b Magnification view

Zn/Mn–sucrose composite, the resultant ZnMnO<sub>3</sub> should well inherit its structure characteristic. Furthermore, the decomposition of sucrose (Fig. 1a) also induces the formation of more porous structure during calcination process [20–22].

The morphologies especially the temperature dependent particle size are further studied in Fig. 3. In a low calcination temperature (Figs. 3a and b), the thick aggregate has obvious inner macroporous structure, consistent with the SEM observation in Fig. 2. The tiny nanoparticles can be found in the edge (Fig. 3b), and some mesopores also can be found between nanoparticles. The porous property of 500°C ZnMnO<sub>3</sub> is further investigated by N<sub>2</sub> adsorption–desorption isotherms and pore size distribution, as shown in Fig. 4. The estimated Brunauer–Emmett–Teller (BET) specific surface area is 25.50 m<sup>2</sup> g<sup>-1</sup> with average pore size of 19.69 nm, and these data should be attributed to its morphology and structure characteristics.

With the calcination temperature increases to 600°C (Fig. 3c), the plate-like aggregate turns to thinner, and the size of above nanoparticles also has been improved, indicating the elevated calcination

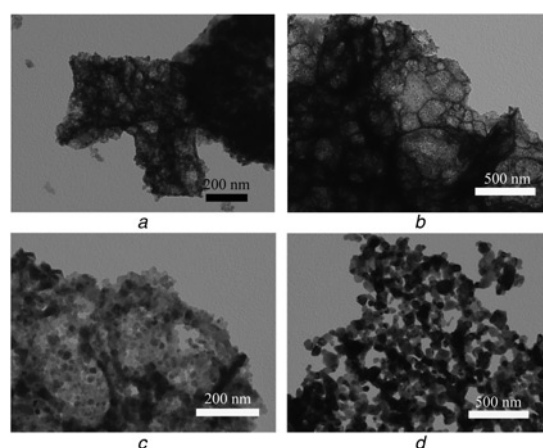


**Fig. 3** TEM images of ZnMnO<sub>3</sub> obtained from different temperatures  
a 400°C  
b 500°C  
c 600°C  
d 700°C

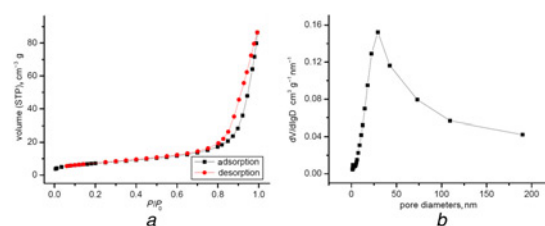


**Fig. 4** Porous property of 500°C ZnMnO<sub>3</sub> is further investigated  
a N<sub>2</sub> adsorption–desorption isotherms  
b Pore size distribution curve of ZnMnO<sub>3</sub> obtained from 500°C

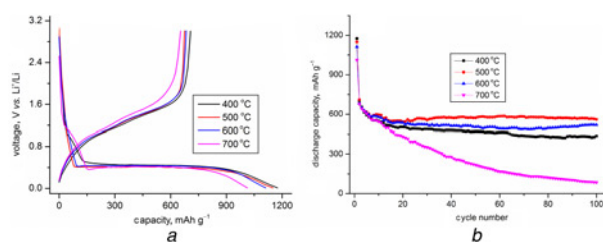


**Fig. 5** Initial discharge charge curves of different  $\text{ZnMnO}_3$  at current density of  $0.4 \text{ A g}^{-1}$   
 a Initial discharge-charge curves  
 b Cycling performances of  $\text{ZnMnO}_3$  obtained from different temperatures at current density of  $0.4 \text{ A g}^{-1}$

temperature has a favour to crystal growth. In Fig. 3d, the size of  $\text{ZnMnO}_3$  nanoparticles can come to  $\sim 100\text{--}150 \text{ nm}$ , and clear corner and edge of nanoparticles indicate this sample should have good crystallinity, agreeing well with the XRD pattern in Fig. 1b.

As far as we know, the lithium storage performances of transition metal oxide anode materials are deeply dependent upon their particle size, porous property and crystallinity. (a) The small particle size can provide short lithium/electron pathway, and helps to improve the discharge capacity. Thus, a smaller particle size means better electrochemical performance, to a great extent. (b) As above mentioned, the porous structure can buffer the volume change during cycling, and the existence of porous structure is helpful to improve electrochemical performances. (c) In comparison, the influences of crystallinity are more complex. The electrode materials with poor crystallinity are difficult to provide solid framework for lithium insertion, resulting in bad cycling stability. Oppositely, the electrode materials with ultra-high crystallinity are difficult to have phase transformation (It should be mentioned out, a complicate structure and phase transformation will happen for conversion-type metal oxides anode) during discharge-charge process, especially initial cycle. These may lead to the pulverisation of electrode materials and low discharge capacity. Thus, a moderate crystallinity may be preferred [3–5, 17].

The as-prepared  $\text{ZnMnO}_3$  from different temperatures have distinct structures and morphologies, and they will show different electrochemical performances as lithium-ion battery anodes. Fig. 5a shows the initial discharge charge curves of different  $\text{ZnMnO}_3$  at current density of  $0.4 \text{ A g}^{-1}$ . The sample obtained from 400, 500, 600 or  $700^\circ\text{C}$  reveals an initial discharge capacity of 1175.5, 1150.6, 1111.9 or  $1012.7 \text{ mAh g}^{-1}$ , and charge capacity of 706.8, 674.8, 683.7 or  $653.8$ , respectively. The initial Coulombic efficiency of all samples is nearby 60%, and the discharge capacity decreases with the elevated temperature. The cycling performances of different samples are revealed in Fig. 5b, the second cycle discharge capacity is 699.8, 709.6, 680.8 or  $676.6 \text{ mAh g}^{-1}$ , after 100 cycles, the residual discharge capacity is 436.3, 560.0, 518.7 or  $85.2 \text{ mAh g}^{-1}$  for the different samples, correspondingly giving the capacity retention of 62.3, 78.9, 76.2 or 12.6%, respectively. It can be obviously found that, the  $\text{ZnMnO}_3$  obtained from  $500^\circ\text{C}$  has higher capacity retention, as well as the highest discharge capacity over 100 cycles. Maybe, the improved electrochemical performance can be attributed to its small particle size, porous nature and moderate crystallinity, as discussed above [17].

The rate capacity retentions of optimal  $\text{ZnMnO}_3$  also are evaluated at different current densities, as shown in Fig. 6. As we expected, the specific capacity decreases from  $730.0 \text{ mAh g}^{-1}$  at  $0.2 \text{ A g}^{-1}$  to  $520.7 \text{ mAh g}^{-1}$  at  $0.8 \text{ A g}^{-1}$ . When the current density increases to  $1.2 \text{ A g}^{-1}$ , the cell delivers an unstable discharge capacity about  $350 \text{ mAh g}^{-1}$ , indicating this sample had better be used within the current density of  $1.0 \text{ A g}^{-1}$ . Importantly, when the current density goes back to  $0.2 \text{ A g}^{-1}$ , the electrode keeps a stable discharge capacity of  $\sim 635.0 \text{ mAh g}^{-1}$ .

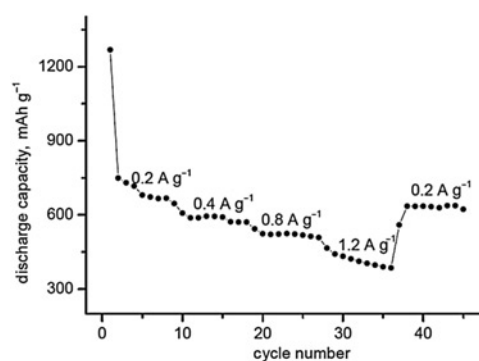


**Fig. 6** Rate capability of  $\text{ZnMnO}_3$  at different current densities

**3. Conclusion:** A facile sucrose assisted route has been developed for the synthesis of porous  $\text{ZnMnO}_3$  plate. The as-prepared  $\text{ZnMnO}_3$  composed of numerous nanoparticles has a BET specific surface area of  $\sim 25.50 \text{ m}^2 \text{ g}^{-1}$  and pore size of  $\sim 19.69 \text{ nm}$ . As lithium-ion battery anodes, the  $\text{ZnMnO}_3$  shows a high discharge capacity and good cycling stability. A discharge capacity of  $560.0 \text{ mAh g}^{-1}$  can be retained after 100 cycles. Maybe, it is a convenient synthesis route, and can be used to prepare other binary metal oxides.

**4. Acknowledgment:** The authors thank the financial supports from the Scientific Start Foundation of LongYan University (LB2014001), and from Provincial Science and Technology Department for Provincial Colleges and Universities Program (JK2015047).

## 5 References

- [1] Poizot P., Laruelle S., Grugeon S., *ET AL.*: 'Nano-sized transition-metal oxides as negative-electrode materials for lithium-ion batteries', *Nature*, 2000, **407**, pp. 496–499
- [2] Deng Y.F., Zhang Q.M., Tang S.D., *ET AL.*: 'One-pot synthesis of  $\text{ZnFe}_2\text{O}_4/\text{C}$  hollow spheres as superior anode materials for lithium ion batteries', *Chem. Commun.*, 2011, **47**, pp. 6828–6830
- [3] Liu R., Yang W.D., Fang H.Y.: 'Performance of  $\text{SnO}_2/\text{carbon}$  nanotube composite electrode materials by the Pechini method', *Micro Nano Lett.*, 2016, **11**, pp. 54–56
- [4] Gao J., Lowe M., Abruna H.D.: 'Spongelike nanosized  $\text{Mn}_3\text{O}_4$  as a high-capacity anode material for rechargeable lithium batteries', *Chem. Mater.*, 2011, **23**, pp. 3223–3227
- [5] Li J.F., Xiong S.L., Li X.W., *ET AL.*: 'Spinel  $\text{Mn}_{1.5}\text{Co}_{1.5}\text{O}_4$  core-shell microspheres as Li-ion battery anode materials with a long cycle life and high capacity', *J. Mater. Chem.*, 2012, **22**, pp. 23254–23259
- [6] Yang Y.Y., Zhao Y.Q., Xiao L.F., *ET AL.*: 'Nanocrystalline  $\text{ZnMn}_2\text{O}_4$  as a novel lithium-storage material', *Electrochem. Commun.*, 2008, **10**, pp. 1117–1120
- [7] Xia L.F., Yang Y.Y., Yin J., *ET AL.*: 'Low temperature synthesis of flower-like  $\text{ZnMn}_2\text{O}_4$  superstructures with enhanced electrochemical lithium storage', *J. Power Sources*, 2009, **194**, pp. 1089–1093
- [8] Zhang G.Q., Yu L., Wu H.B., *ET AL.*: 'Formation of  $\text{ZnMn}_2\text{O}_4$  ball-in-ball hollow microspheres as a high-performance anode for lithium-ion batteries', *Adv. Mater.*, 2012, **24**, pp. 4609–4613
- [9] Zhou L., Wu H.B., Zhu T., *ET AL.*: 'Facile synthesis of  $\text{ZnMn}_2\text{O}_4$  hollow microspheres as high-capacity anodes for lithium-ion batteries', *J. Mater. Chem.*, 2012, **22**, pp. 827–829
- [10] Kim S.W., Lee H.W., Muralidharan P., *ET AL.*: 'Electrochemical performance and *ex situ* analysis of  $\text{ZnMn}_2\text{O}_4$  nanowires as anode materials for lithium rechargeable batteries', *Nano Res.*, 2011, **4**, pp. 505–510
- [11] Zhang Y.H., Zhang Y.W., Guo C.L., *ET AL.*: 'porous  $\text{ZnMn}_2\text{O}_4$  nanowires as an advanced anode material for lithium ion battery', *Electrochim. Acta*, 2015, **182**, pp. 1140–1144
- [12] Deng Y.F., Tang S.D., Zhang Q.M., *ET AL.*: 'Controllable synthesis of spinel nano- $\text{ZnMn}_2\text{O}_4$  via a single source precursor route and its high capacity retention as anode material for lithium ion batteries', *J. Mater. Chem.*, 2011, **21**, pp. 11987–11995

- [13] Wang N.N., Ma X.J., Xu H.Y., *ET AL.*: 'Porous  $\text{ZnMn}_2\text{O}_4$  microspheres as a promising anode material for advanced lithium-ion batteries', *Nano Energy*, 2014, **6**, pp. 193–199
- [14] Rall J.D., Thota S., Kumar J., *ET AL.*: 'Synthesis, structure, and magnetic behavior of nanoparticles of cubic  $\text{ZnMnO}_3$ ', *Appl. Phys. Lett.*, 2012, **100**, p. 252407
- [15] Salaf L.V., Nachimuthu P., Engelhard M.H., *ET AL.*: 'Stabilization of  $\text{ZnMnO}_3$  phase from sol-gel synthesized nitrate precursors', *J. Sol-Gel Sci. Technol.*, 2010, **53**, pp. 141–147
- [16] Liu X.R., Zhao C.H., Zhang H., *ET AL.*: 'Facile Synthesis of porous  $\text{ZnMnO}_3$  spherulites with a high lithium storage capability', *Electrochim. Acta*, 2015, **151**, pp. 56–62
- [17] Zhang L., Wu H.B., Lou X.W.: 'Formation of  $\text{Fe}_2\text{O}_3$  microboxes with hierarchical shell structures from metal-organic frameworks and their lithium storage properties', *J. Am. Chem. Soc.*, 2012, **134**, pp. 17388–17391
- [18] Beji Z., Smiri L.S., Yaacoub N., *ET AL.*: 'Annealing effect on magnetic properties of polyol-made Zn-Ni ferrite nanoparticles', *Chem. Mater.*, 2010, **22**, pp. 1350–1366
- [19] Qiu Y.C., Yang S.H., Deng H., *ET AL.*: 'A novel nanostructured spinel  $\text{ZnCo}_2\text{O}_4$  electrode material: morphology conserved transformation from a hexagonal shaped nanodisk precursor and application in lithium ion batteries', *J. Mater. Chem.*, 2010, **20**, pp. 4439–4444
- [20] Amarilla J.M., Petrov K., Pico F., *ET AL.*: 'Sucrose-aided combustion synthesis of nanosized  $\text{LiMn}_{1.99-y}\text{Li}_y\text{M}_{0.01}\text{O}_4$  ( $M = \text{Al}^{3+}$ ,  $\text{Ni}^{2+}$ ,  $\text{Cr}^{3+}$ ,  $\text{Co}^{3+}$ ,  $y = 0.01$  and  $0.06$ ) spinels characterization and electrochemical behavior at 25 and at 55°C in rechargeable lithium cells', *J. Power Sources*, 2009, **191**, pp. 591–600
- [21] Li K.Y., Lin S.D., Shua F.F., *ET AL.*: 'A rapid combustion route to synthesize high-performance nanocrystalline cathode materials for Li-ion batteries', *CrystEngComm*, 2014, **16**, pp. 10969–10976
- [22] Liu G.Y., Kong X., Wang B.S.: 'Importance of ignition temperature in solution combustion synthesis of  $\text{LiNi}_{0.5}\text{Mn}_{1.5}\text{O}_4$ ', *J. Electrochem. Soc.*, 2014, **161**, pp. A742–A747
- [23] Zhao C.H., Hu Z.B., Zhou Y.L., *ET AL.*: 'Synthesis of  $0.3\text{Li}_2\text{MnO}_3$ – $0.7\text{LiNi}_{1/3}\text{Co}_{1/3}\text{Mn}_{1/3}\text{O}_2$  cathode materials using 3D urchin-like  $\text{MnO}_2$  as precursor for high performance lithium ion battery', *J. Nanopart. Res.*, 2015, **17**, p. 89
- [24] Zhao C.H., Wang X.X., Liu R., *ET AL.*: ' $\beta$ - $\text{MnO}_2$  sacrificial template synthesis of  $\text{Li}_{1.2}\text{Ni}_{0.13}\text{Co}_{0.13}\text{Mn}_{0.54}\text{O}_2$  for lithium ion battery cathodes', *RSC Adv.*, 2014, **4**, pp. 7154–7159